[1]A. Fukuda, Phys. Rev. B 1, 4161 (1970).
[2]A. Fukuda, Sci. Light 13, 64 (1964).
[3]F. Seitz, J. Chem. Phys. 6, 150 (1938).
[4]F. E. Williams, J. Chem. Phys. 19, 457 (1951).
[5]R. S. Knox and D. L. Dexter, Phys. Rev. 104, 1245 (1956).
[6]R. S. Knox, Phys. Rev. 115, 1095 (1959).
[7]S. Sugano, J. Chem. Phys. 35, 122 (1962).
[8]For a comprehensive review of the problem of thallium in alkali halides, see W. B. Fowler, *Physics of Color Centers* (Academic, New York, 1968), Chap. 2, pp. 133–151.
[9]L. Pauling, *The Nature of the Chemical Bond* (Cornell U. P., New York, 1960), pp. 93–98.
[10]C. J. Ballhausen, *Ligand Field Theory* (McGraw-Hill, New York, 1962), pp. 152–179.
[11]C. J. Ballhausen and H. Gray, *Molecular Orbital Theory* (Benjamin, New York, 1965), pp. 92–132.
[12]C. C. J. Roothan, Rev. Mod. Phys. 23, 69 (1951).
[13]L. C. Allen and J. D. Russell, J. Chem. Phys. 46, 1029 (1967).
[14]D. R. Hartree and W. Hartree, Proc. Roy. Soc. (London) 156A, 45 (1936); A. S. Douglas, D. R. Hartree, and W. A. Runciman, Proc. Cambridge Phil. Soc. 51, 486 (1955).
[15]R. S. Mulliken *et al.*, J. Chem. Phys. 17, 1248 (1949).
[16]A. H. Kahn and A. J. Leyendecker, Phys. Rev. 135, A1321 (1964).
[17]F. Seitz, *The Modern Theory of Solids* (McGraw-Hill, New York, 1940), p. 78.
[18]H. Strunz, *Mineralogische Tabellen* (Akademische Verlagsgesellschaft, Leipzig, 1966).
[19]C. E. Moore, *Atomic Energy Levels*, Natl. Bur. Std. Circ. No. 467 (U.S. GPO, Washington, D. C., 1949).
[20]Reference 11, p. 120.
[21]A. Viste and H. B. Gray, Inorg. Chem. 3, 1113 (1964).
[22]Reference 11, p. 118.
[23]L. M. Branscomb, *Advanced Electronics and Electron Physics* (Academic, New York, 1957), p. 43.
[24]M. Wolfsberg and L. Helmholtz, J. Chem. Phys. 20, 837 (1962).
[25]R. S. Mulliken, J. Chem. Phys. 23, 1833 (1955).
[26]A. Honma, Sci. Light 16, 229 (1967).
[27]J. A. Pople and D. L. Beveridge, *Approximate Molecular Orbital Theory* (McGraw-Hill, New York, 1970), Chap. 3.
[28]R. Pariser, J. Chem. Phys. 21, 568 (1953).
[29]A. A. Misetich and T. Buch, J. Chem. Phys. 41, 2524 (1964).
[30]D. Y. Smith, Phys. Rev. 137, A574 (1965).
[31]J. Owen and J. H. M. Thornley, Rept. Progr. Phys. 29, 675 (1966).
[32]W_0 is the one-electron energy difference ΔE between the configurations $(a_{1g}^*)(t_{1u}^*)$ and $(a_{1g}^*)^2$ corrected by the difference $\Delta J = \langle a_{1g}^*(1)\, t_{1u}^*(2) \,|e^2/r_{12}\,| a_{1g}^*(1) t_{1u}^*(2)\rangle - \langle a_{1g}^*(1) a_{1g}^*(2)\,|e^2/r_{12}\,|a_{1g}^*(1) a_{1g}^*(2)\rangle$ between the Coulomb energy corrections to the configurations $(a_{1g}^*)(t_{1u}^*)$ and $(a_{1g}^*)^2$, respectively. The quantity ΔJ has been estimated in the INDO approximation and it is seen that neglecting small terms, ΔJ becomes $\Delta J \simeq [c_1(a_{1g}^*)]^2[c_1(t_{1u}^*)]^2 \times \langle 6s6p|e^2/r_{12}|6s6p\rangle - [c_1(a_{1g}^*)]^4 \langle 6s^2|e^2/r_{12}|6s^2\rangle - (6)^{-1} \times\{[c_2(a_{1g}^*)]^4 - [c_2(a_{1g}^*)]^2[c_2(t_{1u}^*)]^2\}\langle z^2|e^2/r_{12}|z^2\rangle = 0.6$ eV, where the coefficients $c_{1,2}$ are given in Table I, the value $\langle z^2 \mid e^2/r_{12} \mid z^2\rangle = 7.5$ eV above reported has been used, and the values $\langle 6s^2 \mid e^2/r_{12} \mid 6s^2\rangle = 8.19$ eV and $\langle 6s6p \mid e^2/r_{12} \mid 6s6p\rangle = 7.20$ eV have been computed starting from functions (2). Thus, one has $W_0 = \Delta E + \Delta J = 5.9$ eV.
[33]Y. Toyozawa and M. Inoue, J. Phys. Soc. Japan 21, 1663 (1966).
[34]D. E. McCumber, J. Math. Phys. 5, 508 (1964).
[35]Yu. B. Rozenfel'd, B. G. Vekhter, and B. S. Tsukerblat, Zh. Eksperim. i Teor. Fiz. 55, 2252 (1969) [Sov. Phys. JETP 28, 1195 (1969)].
[36]Yu. E. Perlin, Fiz. Tverd. Tela 10, 1941 (1968) [Sov. Phys. Solid State 10, 1531 (1969)].

PHYSICAL REVIEW B VOLUME 3, NUMBER 11 1 JUNE 1971

Coupling Coefficients for the Indirect Nuclear Dipole Interaction in Indium by Nuclear Quadrupole Resonance

J. P. Palmer* and R. R. Hewitt
University of California, Riverside, California 92502
(Received 8 February 1971)

Moment analysis of the NQR spectrum of indium metal is used to measure its isotropic and anisotropic dipolar interactions. The coupling coefficients $\tilde{A}$ and $\tilde{B}$ are measured to be 2.46×10^{-46} and 1.55×10^{-46} erg cm^3, respectively. The measurement of the NQR in In-Sn alloys is described and found to be in qualitative agreement with earlier NMR results.

I. INTRODUCTION

The dipolar interaction between conduction electrons and atomic nuclei provides valuable means for experimental verification of theories concerning conduction electrons. Knight shifts have been the subject of much investigation in this regard.[1] Evaluation of the Knight-shift parameters from the observed data is most easily achieved for systems with cubic crystal structure, or with nuclear spin

$I=\frac{1}{2}$ species, owing to the absence of quadrupolar perturbations. In systems where the nuclear quadrupole interaction exists, there is the alternative of working in the quadrupolar regime where the dipolar perturbations vanish in first order, and the second-order perturbations dominate the observed line shape. The latter perturbations consist of three parts: the direct dipolar interaction between nuclei and the contact (isotropic) and classical (anisotropic) dipolar interactions between conduction electrons and nuclei. These interactions shift the NQR lines and contribute symmetric and asymmetric broadening.

The second-order interaction between nuclear and conduction-electron dipole moments can be transformed, with certain restrictions, to an indirect interaction between nuclei[2,3] which has the form of a first-order interaction. It includes terms corresponding to exchange and classical dipolar interactions, the strengths of which are indicated by coupling coefficients $\tilde{A}$ and $\tilde{B}$. These coefficients are determined by the original dipole interaction between nuclei and conduction electrons.

Abragam and Kambe[4] developed the correlation between the direct dipolar interaction and the NQR line shape for a nuclear-spin-$\frac{3}{2}$ system using the Van Vleck moment analysis technique.[5] Bloembergen and Rowland[3] incorporated the indirect classical dipolar coupling $\tilde{B}$ in an analysis in the NMR regime for the spin-$\frac{1}{2}$ system. The present investigation extends these analyses to include the direct interaction as well as the indirect exchange and classical dipolar interactions for a spin-$\frac{9}{2}$ system in the NQR regime. These results are correlated with measured data for indium to evaluate the coefficients $\tilde{A}$ and $\tilde{B}$.

II. MOMENT ANALYSIS IN THE QUADRUPOLAR REGIME FOR SPIN-$\frac{9}{2}$ NUCLEI

The second-order hyperfine interaction is described formally by the many-body Hamiltonian

$$H' = \sum_{i,j}\left(-\frac{8\pi}{3}\vec{\mu}_{ei}\cdot\vec{\mu}_{nj}\,\delta(\vec{r}_{ij}) + \frac{\vec{\mu}_{ei}\cdot\vec{\mu}_{ni}}{r_{ij}^3} - \frac{3(\vec{\mu}_{ei}\cdot\vec{r}_{ij})(\vec{\mu}_{ni}\cdot\vec{r}_{ij})}{r_{ij}^5}\right), \quad (1)$$

where $\vec{\mu}_{ei}$ and $\vec{\mu}_{nj}$ are conduction-electron and nuclear-dipole moments, and $\vec{r}_{ij}$ is the radius vector between them. First-order perturbation theory applied to Eq. (1) produces the isotropic and anisotropic Knight shifts, as mentioned above. Second-order perturbation theory applied to Eq. (1) reduces to indirect interactions between nuclei, where conduction electrons are polarized by nuclear moments which themselves react to the polarized electrons. The Hamiltonian for this interaction among nuclei is

$$H' = \tilde{A}\sum_{i,i'} R_{jj'}^{-3}\,\vec{I}_j\cdot\vec{I}_{j'} + \tilde{B}\sum_{j,j'} R_{jj'}^{-3} \times[\vec{I}_j\cdot\vec{I}_{j'} - 3R_{jj'}^{-2}(\vec{I}_j\cdot\vec{R}_{jj'})(I_{j'}\cdot R_{jj'})], \quad (2)$$

where $\vec{I}_j$, $\vec{I}_{j'}$ are the spin operators for nuclei j and j', and $R_{jj'}$ is the radius vector between them.

The first and second moments of the NQR line are related to traces of the perturbing Hamiltonian in the manner described in Refs. 5 and 6. It is to be emphasized that whereas the shift in first moment vanishes in the NMR regime, it is finite in the NQR regime. The resulting m dependence of the first- and second-moment expressions is given in Table I. Note in particular that the first-moment shift relative to the quadrupolar frequency has the same m dependence as the pure quadrupolar frequency itself, $\frac{1}{2}(2m+1)\nu_q$,

$$\hbar\langle\Delta\omega\rangle = -(2m+1)[1.44\tilde{A} + 0.74(B+\tilde{B})], \quad (3)$$

where $B=\gamma^2\hbar^2$ is the coupling coefficient for the direct dipolar interaction between nuclei. Therefore, the first moment $\langle\omega\rangle$ also has the m dependence, i.e.,

$$\langle\omega\rangle = \tfrac{1}{2}(2m+1)(2\pi\nu_q + \langle\Delta\omega\rangle_{1/2}). \quad (4)$$

Consequently, empirical determination of $\langle\omega\rangle$ does not resolve directly the quadrupolar frequency and first-moment shift. However, independent determination of ν_q can be provided by NMR. Since there is no first-moment shift due to spin-spin interactions in the magnetic regime, the quadrupolar frequency resulting from the analysis of NMR is an unperturbed frequency. The indium ν_q thus determined by Anderson[7] is $\nu_q = 1.891$ MHz. For the moment expressions used in the calculations, consult Table I.

TABLE I. Moment expressions.

m	$-\hbar\langle\Delta\omega\rangle\times10^{-23}$	$(\hbar^2\langle\Delta\omega^2\rangle+\hbar^2\langle\Delta\omega\rangle^2)\times10^{-46}$
$\frac{1}{2}$	$2.44\tilde{A}+1.48(B+\tilde{B})$	$0.634\tilde{A}^2-0.00562\tilde{A}(B+\tilde{B})+0.0654(B+\tilde{B})$
$\frac{3}{2}$	$4.88\tilde{A}+2.96(B+\tilde{B})$	$0.505\tilde{A}^2-0.00384\tilde{A}(B+\tilde{B})+0.0695(B+\tilde{B})^2$
$\frac{5}{2}$	$7.32\tilde{A}+4.44(B+\tilde{B})$	$0.335\tilde{A}^2-0.00142\tilde{A}(B+\tilde{B})+0.0638(B+\tilde{B})^2$
$\frac{7}{2}$	$9.76\tilde{A}+5.92(B+\tilde{B})$	$0.138\tilde{A}^2+0.000784\tilde{A}(B+\tilde{B})+0.0578(B+\tilde{B})^2$
$\frac{9}{2}$		

III. ZEEMAN BROADENING OF NQR FOR SPIN-$\frac{9}{2}$ NUCLEI

Application of a small static magnetic field perpendicular to the rf coil of an NQR sample splits the m degeneracy of the zero-order levels, which produces broadening in addition to that produced by internal sources. This Zeeman broadening is the basis for the modulated signal received by the phase-sensitive detector of the nuclear resonance spectrometer. The recorded output of the spectrometer is the difference between Zeeman-broadened and the normal NQR lines, where the latter is needed to compare with the moment expressions of Sec. II. In order to obtain the unbroadened line shape, it was necessary to describe the broadened line shape to subtract from the measured shape.

The Zeeman-broadened NQR distribution is represented analytically by the integral

$$Z(\nu)=\int_0^\infty F_Z(\nu-\nu')I(\nu')d\nu' , \tag{5}$$

where $I(\nu)$ is the zero-field NQR distribution, and $F_Z(\nu-\nu')$ is the Zeeman broadening function which represents the distribution originating from the zero-field resonance at ν'. Then, given the Zeeman broadening function, the pure-NQR line shape can be recovered from the integral equation

$$I_{\text{meas}}(\nu)=I(\nu)-\int_0^\infty F_Z(\nu-\nu')I(\nu')d\nu' . \tag{6}$$

where $I_{\text{meas}}(\nu)$ is the measured line shape. The solution can be obtained numerically by applying finite limits to the integral, outside of which $I(\nu)$ is assumed to vanish, writing the integral in matrix notation, and inverting.

The Zeeman broadening function $F_Z(\nu-\nu')$ is derived from a powder pattern analysis since the splitting of degenerate levels by a static magnetic field depends on the relative orientation of the magnetic field and the principle axis of a given crystal. This analysis is given in Ref. 6. The resultant functions are only piecewise analytic and are shown graphically for spin-$\frac{9}{2}$ nuclei in a field of 112 G in Fig. 1. Prior to application in the solution for $I(\nu)$, the broadening function corresponding to the transition of interest must be normalized according to

$$\int_{-\infty}^{\infty} I_{\text{meas}}(\nu-\nu')d(\nu-\nu')=1 , \tag{7}$$

whereby the integral of Eq. (6) over all frequencies vanishes identically.

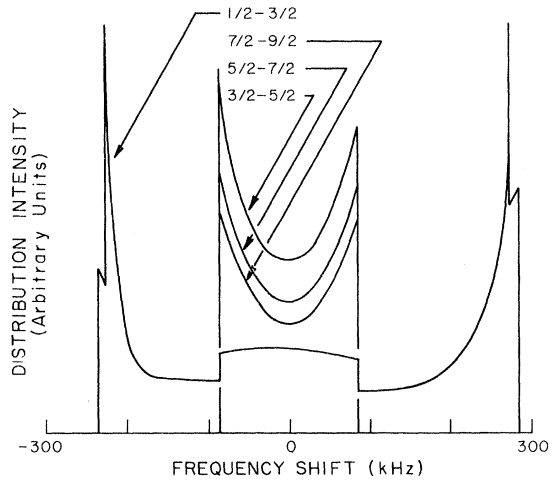

FIG. 1. Zeeman broadening functions for spin-$\frac{9}{2}$ nuclei in an external field of 112 G.

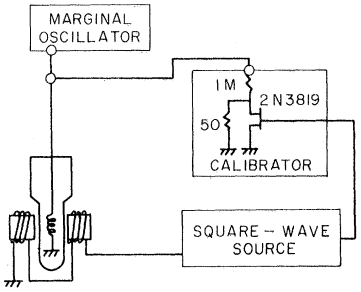

FIG. 2. Schematic diagram of the spectrometer showing the FET calibrator that was developed for the NQR intensity measurements.

IV. EXPERIMENTAL METHOD

All reported measurements were made at 4.2 °K with a nuclear resonance spectrometer employing a marginal oscillator similar to the Pound-Knight oscillator.[8] Radio-frequency power absorbed by the sample is amplitude modulated by a 50-Hz square-wave magnetic field applied to the sample. Detection of the modulated signal produces an audio voltage proportional to the difference in resonance absorption with the field on and off. The resulting audio signal is transmitted to a lock-in amplifier and phase-sensitive detector from which the output level is recorded as the rf frequency is swept slowly through the resonance. A single sweep required about three hours in order to produce absorption curves with negligible phase lag via the 10-sec time constant of the phase-sensitive detector.

Since the spectrometer sensitivity varies over the required sweep ranges, a calibrator was installed in the tank circuit of the marginal oscillator. It consists of a 1-MΩ resistor in series with a field-effect transistor (FET), which is shunted by a 5-Ω resistor as shown in Fig. 2. During calibration, a 10-V bidirectional square wave switches

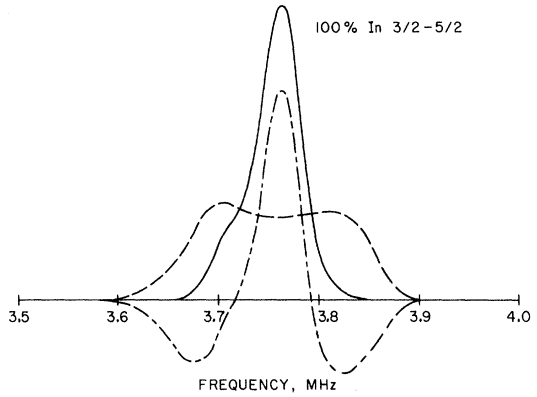

FIG. 3. Demodulation of the measured data.

the FET at the characteristic frequency of the spectrometer producing a conductance modulation of the tank circuit in analogy to that produced by the sample during resonance. The conductance modulation produced by the calibrator is itself frequency dependent and was calibrated by measuring proton magnetic resonances over the required frequency range.

V. RESULTS

Nuclear quadrupole resonances were recorded for 325-mesh, 99.999% indium powder. As-recorded data for the four transitions are shown in Fig. 3. The observed base line drift is ascribed to magnetoresistance where additional rf power is absorbed by conduction electrons. In order to obtain the pure ^{115}In NQR, the following operations were performed: (a) The as-recorded trace was corrected according to the sensitivity calibration of the spectrometer; (b) a smooth base line was interpolated from either side of the resonance; (c) the pure-NQR curve was separated from the Zeeman-broadened resonance (an example of the Zeeman demodulation is shown in Fig. 4); and (d) the

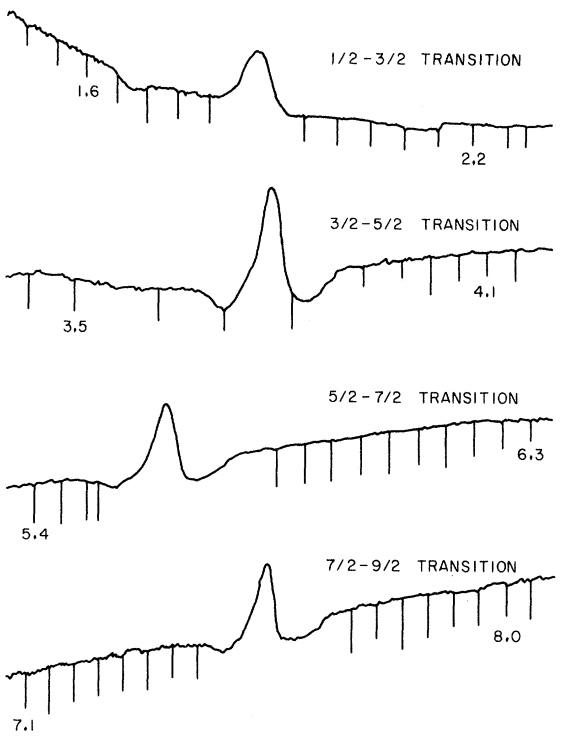

FIG. 4. As-recorded pure indium NQR. Frequencies are in MHZ.

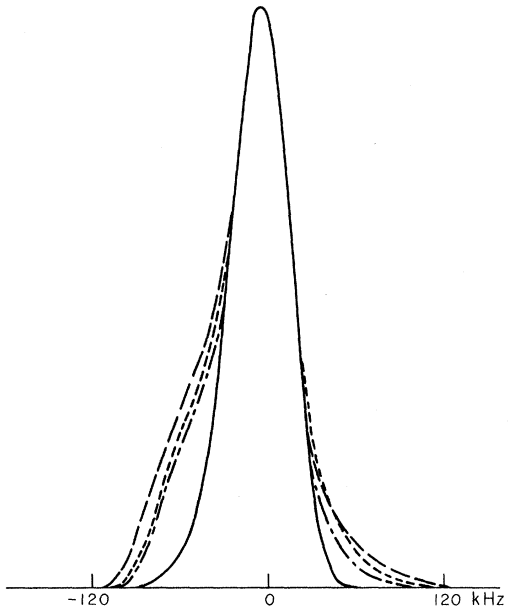

FIG. 5. Pure-NQR curves for pure indium, referenced to frequency of peak intensity. The widths increase with m values.

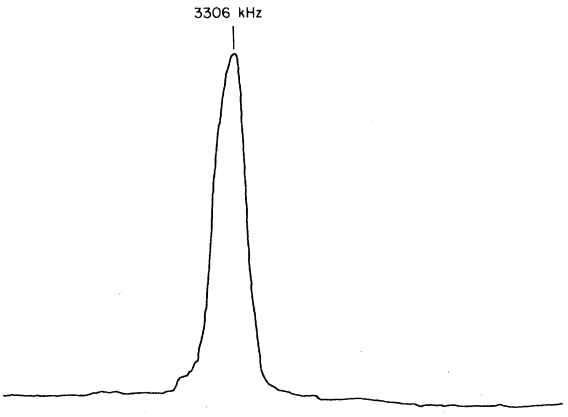

FIG. 6. NQR of nitrogen in hexamethylene-tetramine. Frequency increases to the right.

TABLE II. Line-shape parameters for pure indium NQR.

Transition ($m \rightarrow m+1$)	$\langle \nu \rangle$ (kHz)	Linewidth (FWHM)[a] (kHz)	$\langle \nu \rangle - \frac{1}{2}(2m+1) \times 1891$ (kHz)	$\langle (\nu - \langle \nu \rangle)^2 \rangle$ (kHz)^2	ν_{peak} (kHz)
$\frac{1}{2}$-$\frac{3}{2}$	1872	47	−19	521	1883
$\frac{3}{2}$-$\frac{5}{2}$	3756	49	−26	956	3764
$\frac{5}{2}$-$\frac{7}{2}$	5635	53	−39	1248	5652
$\frac{7}{2}$-$\frac{9}{2}$	7522	51	−42	1096	7537

[a]FWHM = full width at half-maximum.

^{113}In and ^{115}In resonances were separated. The latter separation was achieved by considering the minor, ^{113}In, resonance to be shifted down in frequency by the ratio of the quadrupole moments and by assuming similar line shapes with intensities in the ratio of natural abundances.

The reduced ^{115}In NQR curves are shown in Fig. 5. They have been normalized with respect to absorption intensity and superimposed with respect to frequency of peak intensity. The $\frac{3}{2}$-$\frac{5}{2}$, $\frac{5}{2}$-$\frac{7}{2}$, and $\frac{7}{2}$-$\frac{9}{2}$ curves are almost identical in shape. The $\frac{1}{2}$-$\frac{3}{2}$ transition is significantly lower in intensity in the tail regions. The uniqueness of the latter line shape corresponds to the distinction of that transition in the quantum-mechanical analysis as discussed in Ref. 6.

The asymmetries of the resonances in Fig. 5 are similar to the asymmetry of the nitrogen NQR in hexamethylene-tetramine (HMT) shown in Fig. 6. The latter is shown for comparison since this narrow as-recorded curve is essentially the pure-NQR curve. This is because the HMT resonance is so narrow that the Zeeman-broadened portion is spread into the noise level, and no calibration is required. The low-frequency sides of the resonances have more gradual slopes and show the signs of structure similar to that reported by Scott[9] for solid nitrogen. This is also consistent with the negative shift in first moment due to the spin-spin perturbations discussed above.

Moments and other parameters for the indium NQR curves in Fig. 5 are listed in Table II. The first moments should have the proportionality 1:2:3:4, since the spin-spin perturbations do not affect that proportionality. The weighted mean of the first moments, i.e., the sum of the four first moments divided by 10, is $\langle \overline{\nu} \rangle = 1878$ kHz. The $\frac{3}{2}$-$\frac{5}{2}$ and $\frac{5}{2}$-$\frac{7}{2}$ transitions have first moments in precise proportion to this mean, whereas the first moment of the $\frac{1}{2}$-$\frac{3}{2}$ transition is 6 kHz lower than $\langle \overline{\nu} \rangle$, and that of the $\frac{7}{2}$-$\frac{9}{2}$ transition is 10 kHz higher than $4\langle \overline{\nu} \rangle$.

When the experimental moments for pure indium are used in the expressions for the spin-spin coefficients in Table I, the mean first-moment shift yields the linear relation

$$\tilde{A} + 0.607(B + \tilde{B}) = 3.51 \times 10^{-46} \text{ erg cm}^3 , \quad (8)$$

and the second moment for the $\frac{1}{2}$-$\frac{3}{2}$ transition yields the quadratic relation

$$\tilde{A}^2 - 0.00888\tilde{A}(B + \tilde{B}) + 0.103(B + \tilde{B})^2 = 6.04 \times 10^{-92} \text{ erg}^2 \text{cm}^6 . \quad (9)$$

Simultaneous solution of Eqs. (8) and (9), plotted

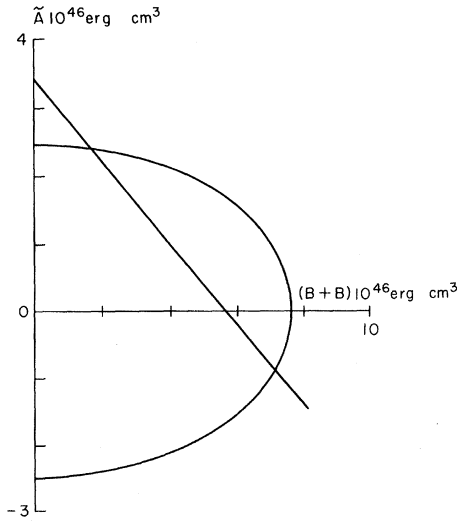

FIG. 7. Simultaneous solution of Eqs. (8) and (9) for the spin-spin coupling coefficients.

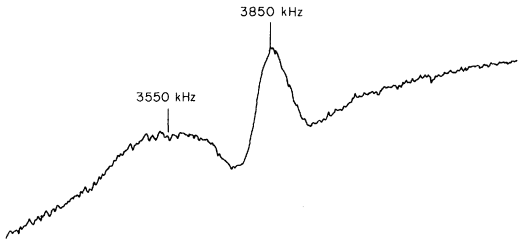

FIG. 8. As-recorded NQR for 99.4% In-0.6% Sn, $\frac{3}{2}$-$\frac{5}{2}$ transition.

in Fig. 7, yields

$$\tilde{A} = 2.40\times10^{-46} \text{ and } \tilde{B} = 1.55\times10^{-46} \quad (10)$$

or

$$\tilde{A} = -0.87\times10^{-46} \text{ and } \tilde{B} = 6.85\times10^{-46}. \quad (11)$$

The present analysis does not specify the correct pair of solutions. This ambiguity is similar to that encountered by Bloembergen and Rowland[3] in their analysis of thallium in the magnetic regime. As they point out, however, the relative strengths of the pseudo-exchange-coupling and the classical dipolar coupling increases from a ratio of 0.01 in the light elements such as the HD molecule to a ratio of 10 to 20 in the heavier metallic elements such as thallium. On this basis, the values $\tilde{A} = 2.40\times10^{-46}$ and $\tilde{B} = 1.55\times10^{-46}$ erg cm^3 are favored for indium. This results in $\tilde{A}/\tilde{B} = 6.8$.

The NQR for dilute alloys of tin in indium have also been measured. The problem of very broad alloy resonances precluded accurate reduction of the measured data since the Zeeman-modulated distribution exceeded the maximum scan width of the spectrometer (for a given marginal oscillator setting). However, the gross asymmetry of the alloy resonances was apparent from the as-recorded data, as seen in Fig. 8, and is in qualitative agreement with the results predicted by Thatcher[10] from his NMR data.

*Present address: California State Polytechnic College, Pomona, Calif. 91766.

[1]See, for example, W. D. Knight, *Solid State Physics* (Academic, New York, 1956), Vol. 2, p. 93.
[2]M. A. Ruderman and C. Kittel, Phys. Rev. 96, 99 (1954).
[3]N. Bloembergen and T. J. Rowland, Phys. Rev. 97, 1679 (1955).
[4]A. Abragam and K. Kambe, Phys. Rev. 91, 894 (1953).
[5]J. H. Van Vleck, Phys. Rev. 74, 1168 (1948).
[6]J. P. Palmer, thesis (University of California, Riverside, 1970) (unpublished).
[7]W. T. Anderson, dissertation (University of California, Riverside, 1964) (unpublished).
[8]R. V. Pound and W. D. Knight, Rev. Sci. Instr. 21, 219 (1950).
[9]T. A. Scott, J. Chem. Phys. 36, 1459 (1962).
[10]F. C. Thatcher, dissertation (University of California, Riverside, 1969) (unpublished); F. C. Thatcher and R. R. Hewitt, Phys. Rev. B 1, 454 (1970).

PHYSICAL REVIEW B VOLUME 3, NUMBER 11 1 JUNE 1971

General Expression for the Density Effect for the Ionization Loss of Charged Particles*

R. M. Sternheimer and R. F. Peierls
Brookhaven National Laboratory, Upton, New York 11973
(Received 21 January 1971)

This paper presents a simple reformulation of the expression for the density effect correction δ, i.e., the reduction in the ionization loss of fast charged particles due to the dielectric polarization of the medium. The general expression for δ thus obtained is applicable to both condensed materials and gases. Its accuracy is such that the resulting values of the ionization loss dE/dx are expected to have a maximum error of less than 2% throughout the range of momenta where the density effect is important.

I. INTRODUCTION

The density effect correction for the ionization loss of charged particles at high energies[1-7] has been previously evaluated for a large number of substances.[4-7] With the advent of the high-energy accelerators in the past decade, the need has arisen for the calculation of the density effect in a variety of additional materials (with various compositions and densities), which were not included in the previous work (Refs. 4–7). In these references, an appropriate dispersion oscillator model was constructed for each new material, and the resulting values of the density effect correction δ as a function of momentum p were then fitted with a four-parameter formula which was first introduced by Sternheimer in 1952. In this formula, δ is actually expressed as a function of X, defined by $X \equiv \log_{10}(p/m_0c)$, where m_0 is the mass of the incident charged particle.

It was recently suggested by Berger[8] that in view of the growing demand for data on $\delta(X)$ for new materials, it would be of interest to obtain a general expression for $\delta(X)$, which would not require a detailed fitting procedure for each substance, if this is possible. After trying several possible fits, we have found such a general expression for the density effect correction $\delta(X)$. The expression